

# Radiation Effects and Defects in Solids

## Incorporating Plasma Science and Plasma Technology

ISSN: 1042-0150 (Print) 1029-4953 (Online) Journal homepage: <http://www.tandfonline.com/loi/grad20>

## Flux trap effect study in a sub-critical neutron assembly using activation methods

K. Routsonis, S. Stoulos, A. Clouvas, N. Catsaros, M. Varvayianni & M. Manolopoulou

**To cite this article:** K. Routsonis, S. Stoulos, A. Clouvas, N. Catsaros, M. Varvayianni & M. Manolopoulou (2016) Flux trap effect study in a sub-critical neutron assembly using activation methods, *Radiation Effects and Defects in Solids*, 171:9-10, 746-753, DOI: 10.1080/10420150.2016.1257620

**To link to this article:** <http://dx.doi.org/10.1080/10420150.2016.1257620>



Published online: 28 Dec 2016.



Submit your article to this journal [↗](#)



Article views: 14




View related articles [↗](#)



View Crossmark data [↗](#)

Full Terms & Conditions of access and use can be found at  
<http://www.tandfonline.com/action/journalInformation?journalCode=grad20>

## Flux trap effect study in a sub-critical neutron assembly using activation methods

K. Routsonis<sup>a</sup>, S. Stoulos <sup>b</sup>, A. Clouvas<sup>c</sup>, N. Catsaros<sup>d</sup>, M. Varvayianni<sup>d</sup> and M. Manolopoulou<sup>b</sup>

<sup>a</sup>INSTN, Centre CEA de Saclay, Saclay, France; <sup>b</sup>Department of Nuclear and Elementary Particle Physics, School of Physics, AUTH, Thessaloniki, Greece; <sup>c</sup>Department of Electrical Energy, School of Electrical and Computer Engineering, AUTH, Thessaloniki, Greece; <sup>d</sup>Institute of Nuclear and Radiological Sciences & Technology, Energy & Safety, NCSR “Demokritos”, Athens, Greece

### ABSTRACT

The neutron flux trap effect was experimentally studied in the sub-critical assembly of the Atomic and Nuclear Physics Laboratory of the Aristotle University of Thessaloniki, using delayed gamma neutron activation analysis. Measurements were taken within the natural uranium fuel grid, in vertical levels symmetrical to the Am–Be neutron source, before and after the removal of fuel elements, permitting likewise a basic study of the vertical flux profile. Three identical flux traps of diamond shape were created by removing four fuel rods for each one. Two ( $n, \gamma$ ) reactions and one ( $n, p$ ) threshold reaction were selected for thermal, epithermal and fast flux study. Results of thermal and epithermal flux obtained through the  $^{197}\text{Au} (n, \gamma) ^{198}\text{Au}$  and  $^{186}\text{W} (n, \gamma) ^{187}\text{W}$  reactions, with and without Cd covers, to differentiate between the two flux regions. The  $^{58}\text{Ni} (n, p) ^{58}\text{Co}$  reaction was used for the fast flux determination. An interpolation technique based on local procedures was applied to fit the cross sections data and the neutron flux spectrum. End results show a maximum thermal flux increase of 105% at the source level, pointing to a high potential to increase in the available thermal flux for future experiments. The increase in thermal flux is not accompanied by a comparable decrease in epithermal or fast flux, since thermal flux gain is higher than epithermal and fast neutron flux loss. So, the neutron reflection is mainly responsible for the thermal neutron increase, contributing to 89% at the central axial position.

### ARTICLE HISTORY


Received 20 September 2016  
Accepted 24 October 2016

### KEYWORDS

Subcritical assembly; neutron flux trap; activation detectors

## 1. Introduction

The standard application in thermal reactors for isotopes production and material testing purposes is to utilize one or more neutron flux traps. These are empty channel positions inside the reactor fuel grid that feature an increased thermal flux for sample irradiations. Since only coolant/moderator exists in a flux trap, it stands that any neutrons that end up in there, simply undergo moderation, without being absorbed by any fuel elements. Due to the moderator, thermal neutrons are also reflected toward the center of the channel and

**CONTACT** S. Stoulos  [stoulos@auth.gr](mailto:stoulos@auth.gr)

accumulate there, hence the name “flux trap”. The ideal position for a flux trap is the center of the fuel grid, where simple neutronics dictate that the flux is at its maximum. The Bessel  $J_0$  function approximates the flux profile of a symmetric fuel grid quite successfully (1–3).

The challenge presented in this experiment is the study of the “flux trap” effect in case of a subcritical assembly and more specifically the subcritical nuclear assembly-reactor, Model 9000 Nuclear Chicago that is installed and operating at the Atomic and Nuclear Physics Laboratory of Aristotle University of Thessaloniki. The subcritical assembly relies on a  $^{241}\text{Am}$ –Be ( $\alpha, n$ ) source at its center, cylindrical natural uranium rods as fuel and light (tap) water as moderator and reflector. It is operating as a student training reactor with  $k_{\text{eff}} = 0.842$  (4). The use of a flux trap with the ultimate goal to provide an increased thermal flux for future experiments has not been yet assessed for the specific assembly.

Therefore, the vertical flux profile of the subcritical assembly both in normal fuel and in “flux trap” configuration was determined. Two ( $n, \gamma$ ) reactions and one ( $n, p$ ) threshold reaction were selected for thermal, epithermal and fast flux study. Results of thermal and epithermal neutrons flux obtained through the  $^{197}\text{Au} (n, \gamma) ^{198}\text{Au}$  and  $^{186}\text{W} (n, \gamma) ^{187}\text{W}$  reactions, with and without Cd covers, to differentiate between the two flux regions. The  $^{58}\text{Ni} (n, p) ^{58}\text{Co}$  reaction was used for the fast neutrons flux estimation. Normally, the vertical flux profile can be described by a simple cosine function, its maximum at the center of the core. However, the presence of the Am–Be source shapes the flux profile, so both the  $J_0$  approximation and the cosine approximation can be used in the case of the subcritical assembly and so there is merit in determining the vertical profile experimentally.

## 2. Experimental

Two sets of irradiations were performed, one with the assembly in regular configuration and one within the flux traps. The irradiation positions were at a constant radial distance of  $28 \pm 0.5$  cm from the centerline and they covered 7 vertical positions, axially symmetrical to the Am–Be source. Three identical flux traps of diamond shape were created by removing four fuel rods for each one. The geometries are presented in Figure 1. Due to the relatively low neutron flux; thick metal discs were used instead of thin foils (see Table 1). The  $^{197}\text{Au} (n, \gamma) ^{198}\text{Au}$ ,  $^{186}\text{W} (n, \gamma) ^{187}\text{W}$  reactions, with and without Cd covers, were used to study the thermal and epithermal flux and the  $^{58}\text{Ni} (n, p) ^{58}\text{Co}$  reaction for fast flux study. Depending on the half-life of the isotope produced, irradiations were last up to four half-lives concerning Au and W samples, while Ni irradiations last up to 1/2 half-lives of  $^{58}\text{Co}$ .

Delayed gamma neutron activation analysis was used to determine the various neutron fluxes  $\Phi$ . The basic principle expression is given in in the following equation:

$$SA = N \cdot \sigma_{\text{eff}} \cdot \Phi, \quad (1)$$

where  $N$  is the nuclei of the target-foil used,  $\sigma_{\text{eff}}$  the effective cross section of the reaction and  $SA$  the saturated activity at the end of the irradiation. The term that can be calculated relatively easily is  $N$ , if one knows the exact composition of the target material. The other terms require a significant amount of work that involves both experimental ( $SA$ ) and modeling approaches ( $\sigma_{\text{eff}}$ ) (5).

The saturated activity  $SA$  was derived by studying the radioactive decay of the desired isotope in the activated sample. Gamma ray measurements were taken in an HPGe detector

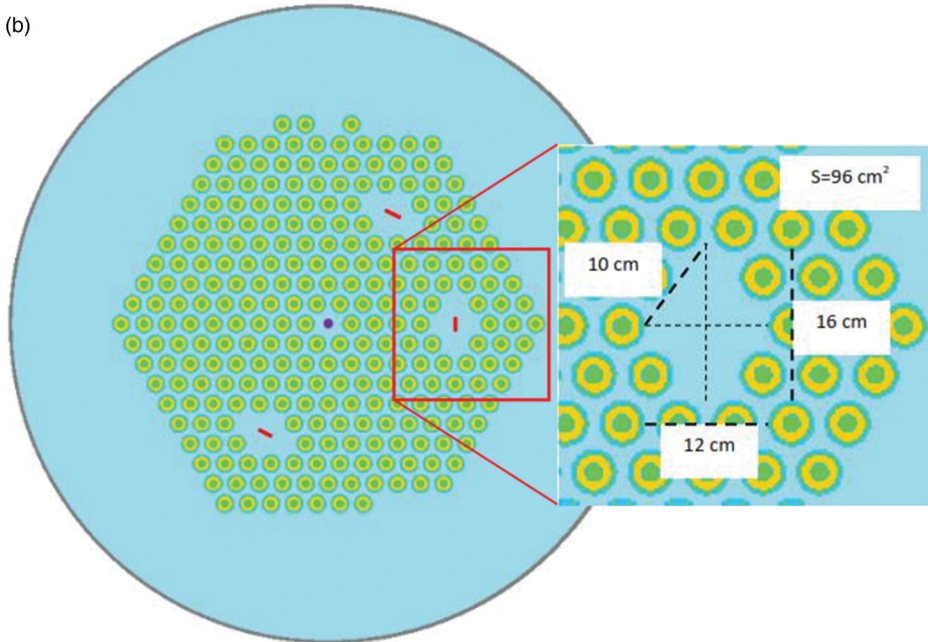
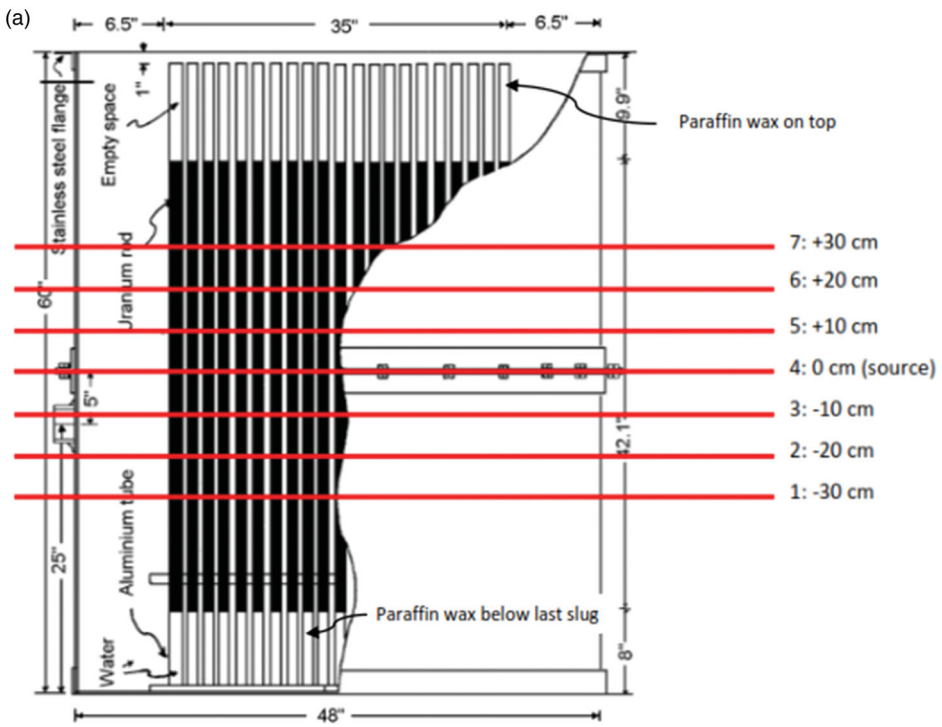


**Figure 1.** (a) Irradiation positions setup for vertical neutron flux measurements. The cross section of the subcritical assembly is presented at the background. (b) The “Flux trap” positions setup in the subcritical assembly-reactor.

**Table 1.** Characteristics of the thick foils applied to the experiment.

Element	Density (g/cm <sup>3</sup> )	Purity	Thickness (mm)	Dimensions (cm)	Mass (gr)
Au	19.30	0.995	0.25	1 × 1	0.4
W	19.30	0.9995	1.00	1 × 1	3.0
Ni	8.91	0.995	2.00	5 × 5	48.0

of 42% relative efficiency and a resolution of 1.8 keV at 1332 keV. The spectra acquisition was done with the winTMCA32<sup>®</sup> software and spectral analysis with the SPECTRW software (6).

In the case of sufficient irradiation time and multiple measurements, the SA has been calculated through fitting of the analysis results. Otherwise, the following expression was used considering only the measurements with dead time lower than 10% of the real time:

$$SA = \frac{\lambda \cdot \text{Net} \cdot (t_{\text{Real}}/t_{\text{Live}})}{(1 - e^{-\lambda \cdot t_i}) \cdot e^{-\lambda \cdot t_d} \cdot (1 - e^{-\lambda \cdot t_{\text{Real}}}) \cdot I_\gamma \cdot \varepsilon'} \quad (2)$$

where Net is the photopeak area,  $t_i$ ,  $t_d$ ,  $t_{\text{Real}}$  and  $t_{\text{Live}}$  are the irradiation, decay, measurements real and live time, respectively;  $\lambda$  is the decay constant,  $I_\gamma$  is the gamma ray intensity and  $\varepsilon$  is the detector efficiency for the particular sample geometry, composition, gamma ray energy, photon self-absorption and coincidence summing. The correction in the intensity of the gammas because of coincidence, the self-absorption of the gammas into the material, the geometry factor and the efficiency of the detector was calculated using GEANT4 simulations. Moreover, corrections on the self-shielding of the neutrons into the foils were also estimated (7).

The next term to be calculated is the effective cross section for the reaction of interest. Since the neutrons that initiate the reaction cover a spectrum of energies and that spectrum is system dependent, the expression used to calculate the effective cross section is

$$\sigma_{\text{eff}} = \frac{\int_{E_1}^{E_2} \sigma(E) \cdot \frac{d\Phi}{dE} dE}{\int_{E_1}^{E_2} \frac{d\Phi}{dE} dE} \quad (3)$$

The excitation function  $\sigma(E)$  data are taken from the ENDF-VII.1 and the  $d\Phi/dE$  quantity, called differential neutron flux (see Figure 2), was taken into account applying the results obtained during a previous study. In the specific study the neutron spectrum has been estimated using a multi-disc neutron activation technique. Fifteen elements have been irradiated and 38 reactions ( $n, \gamma$ ), ( $n, p$ ) and ( $n, \alpha$ ) in total were determined taking into account the gamma self-absorption as well as the neutron self-shielding correction factors due to the disk thickness. The specific activities calculated were the input to the SANDII code, which was built specifically for the neutron spectrum de-convolution when the neutron activation technique is used (8). An interpolation technique based on local procedures was implemented to model the data. Polynomial curves were fitted between every pair of data points and combined in a machine-stored piecewise function (9). The method provides a fast and easy solution, and was successfully validated using the ENDF-VII.1 library (see Figure 3).

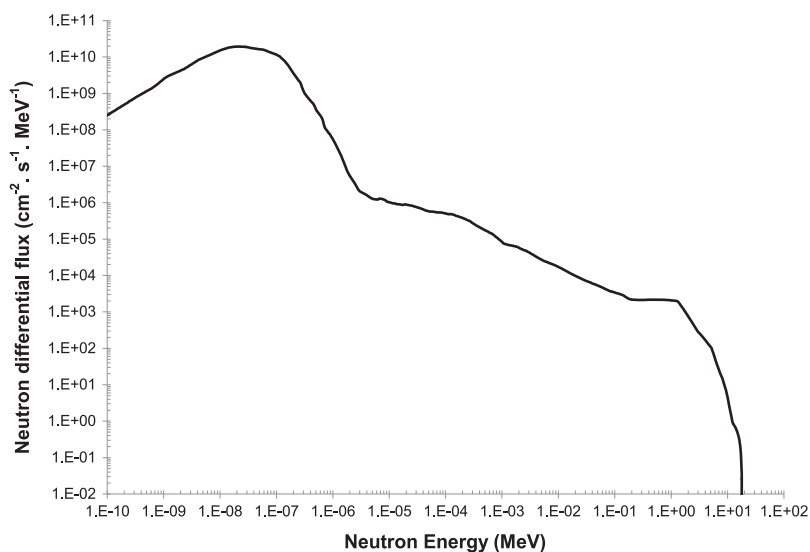


**Figure 2.** Differential neutron flux inside the “flux trap” estimated in previous experiment (8).

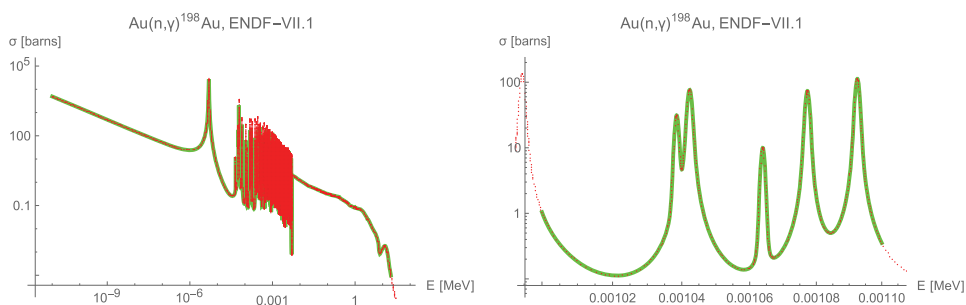


**Figure 3.** Modeling of the  $^{197}\text{Au}(n, \gamma)$  cross section, over the entire spectrum and between 1 and 1.1 keV.

### 3. Results and discussion

The effective cross sections used for experimental data evaluation are presented in Table 2, while the flux results obtained, after all correction factors applied are graphically presented in Figure 4 (thermal neutrons) and Figure 5 (fast and epithermal neutrons). Thermal and fast neutron fluxes are one order of magnitude higher than epithermal neutron flux for both

**Table 2.** Effective cross sections used for experimental data evaluation.

Reaction	Neutron energy range	$\sigma_{\text{eff}}$ (b)
Au-197 ( $n, \gamma$ ) Au-198	Thermal neutrons < 0.5 eV [Cd uncovered – Cd covered foil]	$67.5 \pm 12.4$
	Epithermal neutrons 0.5 eV–10 keV [Cd covered foil]	$156 \pm 35$
W-186 ( $n, \gamma$ ) W-187	Thermal neutrons < 0.5 eV [Cd uncovered – Cd covered foil]	$25.7 \pm 5.1$
	Epithermal neutrons 0.5 eV–10 keV [Cd covered foil]	$48.8 \pm 10.6$
Ni-58 ( $n, p$ ) Co-58	Fast neutrons 0.5–20 MeV	$0.077 \pm 0.019$

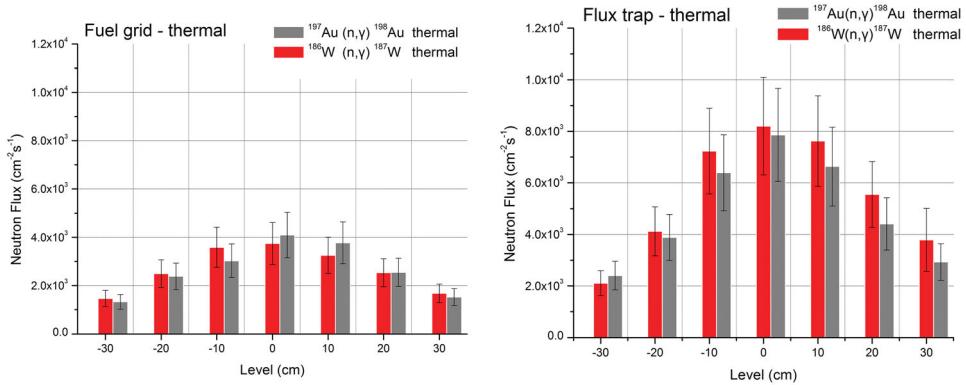


**Figure 4.** Thermal flux results in the fuel grid (left) and the traps (right).

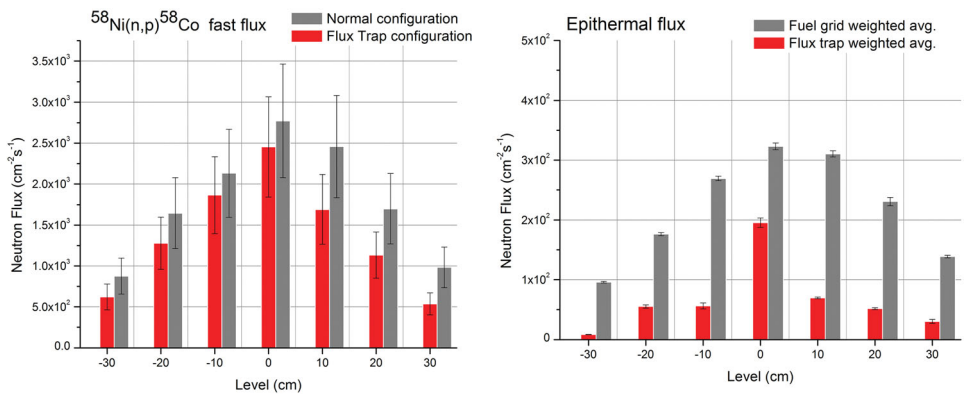


**Figure 5.** Fast (left) and epithermal (right) flux results in the fuel grid and the traps.

configurations (regular and flux traps). The regular configuration of the subcritical assembly produces a double amount of thermal neutrons comparing to the fast ones at distance  $28 \pm 0.5$  cm from the Am–Be neutron source. Moreover, a symmetrical shape of neutron flux across the distance from the source is presented regarding all neutron energy ranges studied.

Inside the “flux traps” only fast neutrons present the same symmetrical behavior. Thermal neutrons flux across all irradiation cycles exhibits lesser fluxes at the two lower positions, ranging from 15% to 40%, compared to their axisymmetrical ones near the water–air interface (see Figure 1(a)). The epithermal neutron flux measurements demonstrate a considerably reduction away from the Am–Be source level.

Thermal neutrons flux inside traps shows an average increase of  $\sim 100\%$  across all positions with the exception of the two lower ones where an increase of  $\sim 50\%$  is estimated. The central axial position yields the maximum thermal neutron flux, from a weighted average  $3.91 \pm 0.52 \times 10^3 \text{ cm}^{-2} \text{ s}^{-1}$  at normal configurations to an average flux  $8.02 \pm 1.10 \times 10^3 \text{ cm}^{-2} \text{ s}^{-1}$  in case of the flux traps, increase 105%.

Epithermal neutron flux decreases  $\sim 80\%$  across all positions inside the trap except the central axial position, where the maximum epithermal neutron flux was obtained.

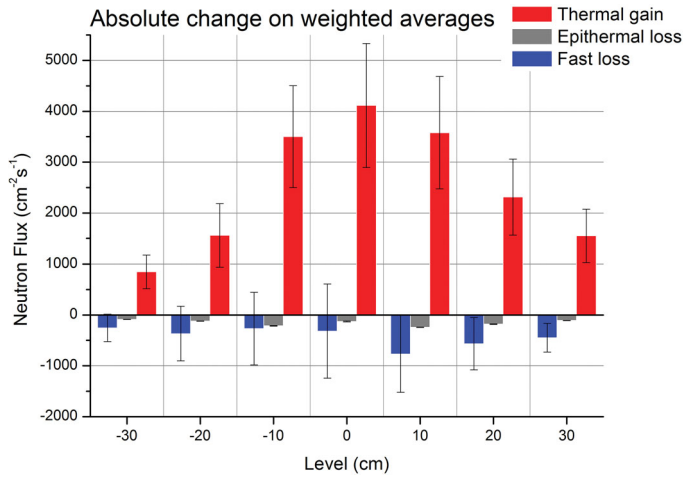


**Figure 6.** Absolute changes in neutron flux due to flux trap effect.

At this position, an average flux  $3.22 \pm 0.62 \times 10^2 \text{ cm}^{-2} \text{ s}^{-1}$  at normal configurations and  $1.92 \pm 0.32 \times 10^2 \text{ cm}^{-2} \text{ s}^{-1}$  in the case of the flux traps was measured corresponding to the minimum decrease 39% observed. The actual gain of thermal neutron due to epithermal neutron loss ranged  $\sim 8\%$  due to the one order of magnitude lower epithermal flux compared to thermal one.

Fast neutrons flux inside traps shows a decrease ranging from 10% up to 42% across all positions. At the central axial position, an average flux  $2.75 \pm 0.49 \times 10^3 \text{ cm}^{-2} \text{ s}^{-1}$  at normal configurations and  $2.48 \pm 0.47 \times 10^3 \text{ cm}^{-2} \text{ s}^{-1}$  in the case of the flux traps was measured resulting in the minimum decrease 10% observed. The maximum decrease 42% is observed at the upper position near the water–air interface.

Thermal flux gain is higher than epithermal and fast neutron flux loss (see Figure 6) so the mainly reason for the thermal neutron increase inside traps is neutron reflection, contributing 89% at the central axial position (see Figure 7). The effect is decreased with distance

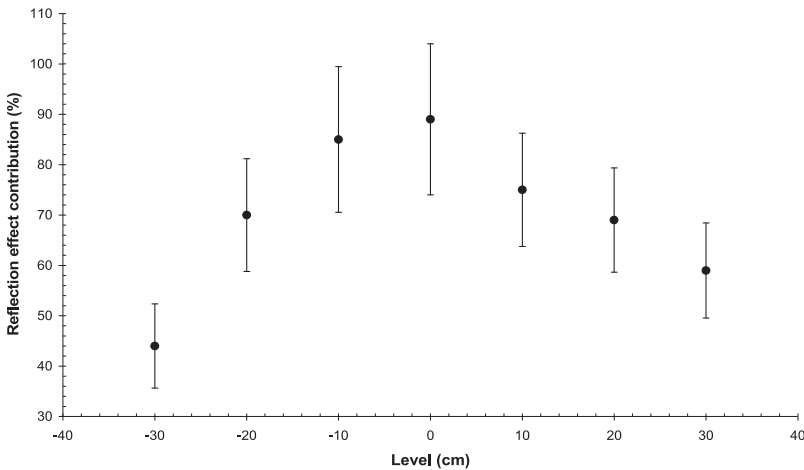


**Figure 7.** Neutron reflection contribution to thermal neutron increment inside the “flux traps”.



increment from the source due to the increase in the neutron leakage. The lower reflection contribution of 44% was measured at the lower position while at its axisymmetrical one, near the water–air interface, a contribution of 59% was estimated demonstrating that the upper irradiation positions benefit from axial reflection, contrary to the lower ones.

#### 4. Conclusions

The neutron flux trap effect was experimentally studied in the subcritical assembly of the Atomic and Nuclear Physics Laboratory of the Aristotle University of Thessaloniki, using delayed gamma neutron activation analysis. Two sets of irradiations were performed, one with the assembly in regular configuration and one within the flux traps. The irradiation positions were at a constant radial distance of  $28 \pm 0.5$  cm from the centerline where the Am–Be source is located. Three identical flux traps of diamond shape were created by removing four fuel rods for each one.

The flux traps designed were found to increase the usable thermal neutron flux by a considerable amount (+105%) in the source axial level, making the practice viable for future irradiation projects and showcasing the high contribution of the reflection effect in flux trap designs. It would be interesting to perform further experiments of this nature in order to properly utilize the flux trap effect and actually achieve higher thermal flux than anywhere in the regular configuration of the subcritical assembly.

#### Disclosure statement

No potential conflict of interest was reported by the authors.

#### ORCID

S. Stoulos  <http://orcid.org/0000-0002-2782-0709>

#### References

- (1) Knief, R. Nuclear Reactor Theory, FSC-6910, DOE-HDBK-1019/2-93, **1993**.
- (2) Khalafi, H.; Gharib, M. *Ann. Nucl. Energy* **2005**, *32*, 331–341.
- (3) Savva, P.; Chatzidakis, S.; Varvayanni, M.; Ikononopoulos, A.; Chrysanthopoulou, N.; Catsaros, N.; Antonopoulos-Domis, M. *Nucl. Technol.* **2014**, *188* (3), 322–335.
- (4) Young, P.-S. *Experiments for Nuclear-Chicago Student Training Reactor*; Nuclear Chicago Corporation: Chicago, IL, **1959**.
- (5) Stoulos, S.; Fragopoulou, M.; Adloff, J.C.; Debeauvais, M.; Brandt, R.; Westmeier, W.; Krivopustov, M.; Sosnin, A.; Papastefanou, C.; Zamani, M.; Manolopoulou, M. *Appl. Radiat. Isot.* **2003**, *58*, 169–175.
- (6) Kalfas, C.A.; Axiotis, M.; Tsabaris, C. *Nucl. Instrum. Methods A* **2016**, *830*, 265–274.
- (7) Vagena, E.; Stoulos, S.; Manolopoulou, M. *Nucl. Instrum. Methods A* **2016**, *806*, 271–278.
- (8) Koseoglou, P.; Vagena, E.; Stoulos, S.; Manolopoulou, M. Neutron spectrum determination in a subcritical assembly using multi-disc neutron activation technique. *Rad. Eff. Def. Solids*, under review.
- (9) Akima, H. *J. ACM* **1970**, *17*, 589–602.